Reprinted from

APPLIED PHYSICS EXPRESS

Influence of Femtosecond Laser Pulse Number on Spike Geometry of Microstructured Silicon

Yan Peng, Miao Hong, Yunyan Zhou, Dan Fang, Xiangqian Chen, Bin Cai, and Yiming Zhu

Appl. Phys. Express **6** (2013) 051303

© 2013 The Japan Society of Applied Physics

Person-to-person distribution (up to 10 persons) by the author only. Not permitted for publication for institutional repositories or on personal Web sites.

Applied Physics Express **6** (2013) 051303
http://dx.doi.org/10.7567/APEX.6.051303

Influence of Femtosecond Laser Pulse Number on Spike Geometry of Microstructured Silicon

Yan Peng, Miao Hong, Yunyan Zhou, Dan Fang, Xiangqian Chen, Bin Cai, and Yiming Zhu*

Engineering Research Center of Optical Instrument and System, Ministry of Education, Shanghai Key Lab of Modern Optical System, Institute of Optical-Electrical Engineering, University of Shanghai for Science and Technology, Shanghai 200093, China
E-mail: py@usst.edu.cn; ymzhu@usst.edu.cn

Received March 24, 2013; accepted April 16, 2013; published online May 7, 2013

We experimentally found that there is an approximately linear relation between the average height/interval distance of spikes and the number of injected femtosecond laser pulses for the pulse number below a threshold. The growth rate of the spike height as a function of the irradiated pulse number is dependent on the gas pressure. When the pulse number exceeds the threshold, a hole can be observed on the silicon surface. Furthermore, the depth of the hole increases with the increase of pulse number. These results are important for optimizing the surface microstructure for silicon-based solar cell fabrication. © 2013 The Japan Society of Applied Physics

Various microstructures can be fabricated when we irradiate femtosecond laser pulses on a single-crystal silicon surface. These microstructures can change the properties of silicon material dramatically.[1,2] Particularly, the light absorption property in the infrared range (>0.8 μm) can be remarkably enhanced to more than 90%,[3,4] which can be widely utilized in various applications, such as solar cells,[5] terahertz emission,[6] negative refraction of light,[7] and optoelectronic detectors.[8–11] Therefore, many efforts have been devoted to the fabrication of microstructured silicon with different surface morphologies for the larger photoelectric absorption coefficient, including the laser fluence,[12] pulse width,[13,14] polarization,[15] pulse number,[16] wavelength,[17] ambient gas,[18] and gas pressure.[19]

However, up to now, the related investigations are mainly focused on the fabrication conditions or laser parameters, and rarely on the spike geometry. The spike geometry includes the spike height and interval distance, which are also important for the final aim: the improvement of the efficiency of the solar cell system. Therefore, in this paper, we experimentally investigated the spike geometry of microstructures as a function of laser pulse number. We find that the average height and distance of conical spikes increase near linearly as the laser pulse number increases until the pulse number exceeds a threshold, when a large hole can be observed. Additionally, the growth rate of the spike height as a function of pulse number is dependent on the gas pressure. We believe that these results are beneficial for the optimal fabrication of microstructures and the later applications of photoelectric devices.

The experimental setup is shown in Fig. 1(a). The laser pulses were produced by a Ti:Sapphire regenerative amplifier, typically 800 nm, 1 kHz, and 45 fs, and the spatial profile of the laser beam energy distribution has a nearly Gaussian shape. The laser beam was focused with a convex lens ($f = 100$ cm), and delivered into a vacuum chamber through a quartz window of 0.4 mm thickness. The vacuum chamber was fixed on a three-axis translation stage to realize the three-dimensional movement and backfilled with SF_6 (the base pressure was less than 10^{-4} Torr). The silicon wafer (phosphor-doped n-type silicon wafer, resistivity: 0.01–0.02 Ω·cm) was mounted in the vacuum chamber and its (100) face was placed vertically toward the incident direction of the laser pulses. The laser spot on the sample surface was monitored with a CCD beam profiler (WinCamD-UCD12) and the diameter of each spot was set

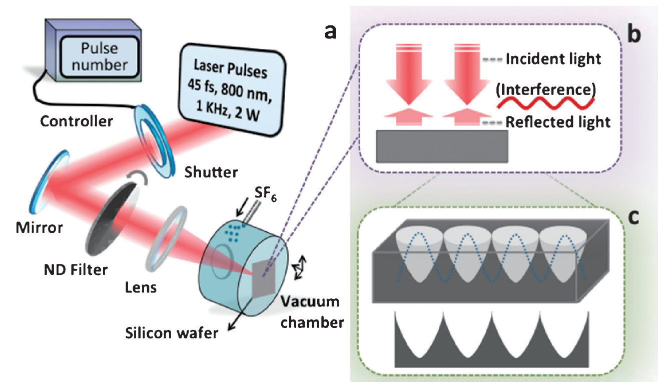

Fig. 1. (a) Apparatus for surface microstructured silicon fabricated using 800 nm femtosecond laser pulses. (b) Schematics of interference between the incident light and reflected light. (c) Energy distribution in the inner of the sample (top) and formed conical spikes (bottom).

at about 400 μm in the entire experiments by adjusting the distance between the silicon wafer and the laser focus. Furthermore, we used a circular variable metallic neutral density (ND) filter to adjust the intensity of the incident laser beam. The pulse number was controlled by a beam shutter (Thorlabs SH05). After irradiation, the surface morphologies of the samples were observed and analyzed by using a scanning electron microscope (SEM; Tescan VEGA II).

The injected laser fluence was set at 0.8 J/cm^2 per pulse during the entire experiment. (The corresponding ablation threshold fluence of Si here was about 0.1 J/cm^2.) Then we investigate the evolution of the microstructure morphology on the silicon surface as a function of pulse number; the corresponding SEM images are shown in Fig. 2. The gas pressure was chosen as 80 kPa here.

We can see that when the pulse number was set to 30, the surface morphology of laser-irradiated area was a quasi-periodic array of bead like structures [Fig. 2(a)]. When the pulse number was increased to 60, the shape of the spike structures started to form gradually [Fig. 2(b)], and when the pulse number was increased to 300, typical conical spikes were observed [Fig. 2(c)]. The average height of the spikes increased continually as we increased the pulse number [Figs. 2(d)–2(g)], until the pulse number exceeded a threshold (here, the threshold is 2700 pulses for the laser power of 1 W). In that case, a hole appeared at the irradiated center of the laser spot on the silicon wafer [Figs. 2(h) and 2(i)].

To show the exact relation between spike geometry and pulse number, we measured the average spike height and

 © 2013 The Japan Society of Applied Physics

Person-to-person distribution (up to 10 persons) by the author only. Not permitted for publication for institutional repositories or on personal Web sites.

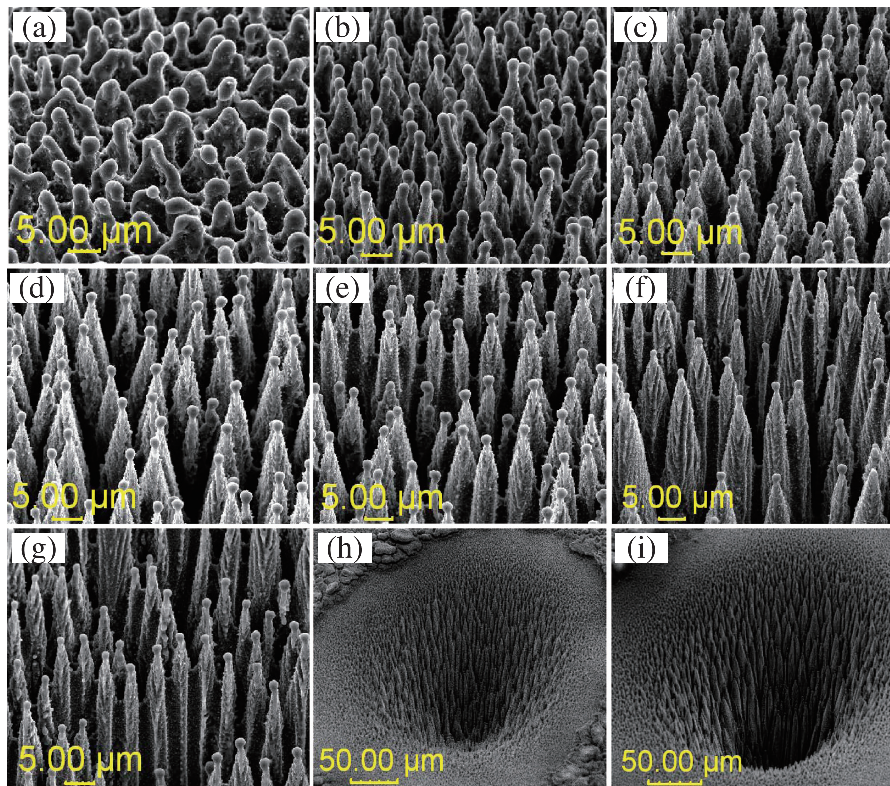

Fig. 2. Scanning electron microscopy images of a silicon surface after femtosecond laser irradiation with the following number of pulses: (a) 30, (b) 60, (c) 300, (d) 900, (e) 1500, (f) 2100, (g) 2700, (h) 3000, and (i) 4200. Each SEM image is taken at a 45° angle to the surface. The laser power is fixed at 1000 mW.

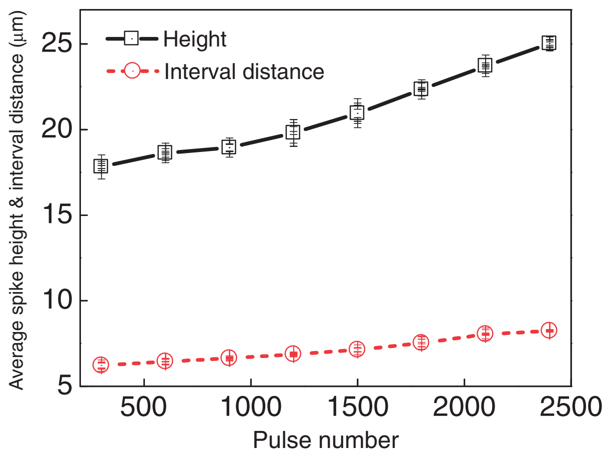

Fig. 3. Average spike height (black solid line) and spike distance (red dashed line) as functions of pulse number. The corresponding error bars have also been shown.

interval distance for each pulse number, as shown in Fig. 3 (The measurement was done by the SEM. The spike height and the interval distance were the average results of 5 points respectively at each corresponding pulse number, and the measuring error was $\sim$1 µm. The interval distance (the distance between two neighboring spikes) was read from the SEM picture directly. For the spike height, a factor of $\sqrt{2}$ was multiplied because the sample was titled 45° angle for the measurement.). It can be seen that the average spike height and distance increase near-linearly after the spike structure is typically formed at the pulse number of 300. Differently, the increase rate of the spike height is quicker than that of the spike distance.

The formation mechanism of the entire process above can be explained from two aspects. Firstly, consider from the microscopic view: when the incident beam irradiates on the mirror surface of single crystal silicon, part of the light can be reflected and then interferes with the incident beam [as shown in Fig. 1(b)], which results in a strong-weak energy distribution pattern on the topmost layer.[20] Then, the silicon wafer absorbs the deposited energy from each pulse. As the absorbed energy exceeds both the ablative and melting thresholds for silicon, chemical reactions between silicon and SF_6 occur at a nonuniform depth,[21] creating capillary waves with the period of laser wavelength. Then, rapid solidification subsequently freezes the capillary structure in place. For the later incident laser pulses, interference cannot be formed on this rough surface again, but the incident laser energy promotes the ablation and melt of materials along the shape of the structure. Then these capillary waves gradually become ripples, then quasi-periodic array of beads and conical spikes. We note that, because the initial strong-weak energy deposition on the silicon surface shows a regular distribution pattern of interference, the energy deposition regions corresponding to the wave crest absorb more energy to promote the ablation of the material; while the energy deposition regions corresponding to the trough of the wave absorb less energy, then, the ablation of the material is not obvious. Finally, the entire material ablation also shows a pattern of interference, i.e., the formed spikes are near conical and the distances between spikes are uniform. The schematic of the energy distribution in the inner part of

 © 2013 The Japan Society of Applied Physics

Person-to-person distribution (up to 10 persons) by the author only. Not permitted for publication for institutional repositories or on personal Web sites.

the sample and the formed spike shape are shown in Fig. 1(c).

Considering the entire process of spike formation, the laser power determines the ablation and volatilization degree of the silicon, while the pulse number represents the interaction time between the laser and silicon, which determines the depth of laser energy transferred into the material interior. Therefore, for the fixed laser power, the silicon material has a stable rate of ablation and volatilization. When the pulse number gradually increases, the linearly increased laser energy determines that the average spike height should also be a nearly linear increase, as shown in Fig. 3 (black solid line). At the same time, when the laser energy is continuously transferred to the deep part of the silicon along the vertical direction, the materials along the horizontal direction are also affected, i.e., ablated and melted. It is just that the horizontal direction is not the main direction of energy transfer; thus, the ablation rate is much slower. As a result, the average spike distance increases linearly but slowly as the pulse number increases, as shown in Fig. 3 (red dashed line).

On the other hand, consider from the macroscopic view: the spatial profile of the entire irradiated laser beam has a Gaussian shape, i.e., the energy distribution at the beam center is the highest, and then the transverse energy distribution is well approximated by the Gaussian function. At the same time, we have known that the higher the laser energy, the higher the ablation and volatilization rate of the silicon material. Therefore, when the Gaussian-shaped laser beam is incident on the silicon surface, the distribution of the material ablation is also Gaussian-shaped, i.e., the material in the center ablates quicker than that in the surrounding. This induces a hole to be formed in the center of the irradiated area. At first, the depth of the hole is too shallow to be observed. While as the number of irradiated pulse increases, the depth of the hole gradually increases and, finally, the hole [Fig. 2(h)] can be clearly observed [Fig. 2(i)]. At this moment, the average height of spikes cannot be measured exactly again because the bottom of the hole is different to distinguish. Certainly, if the pulse number of the femtosecond laser increases further, the depth of the hole can become deeper, and we think that the average height of the spikes is still increasing. By measuring the absorption of the sample in 200–2500 nm (Lambda 750s UV/Vis/NIR spectrophotometer, Perkin Elmer), we found that the formation of holes cannot further promote the light absorption, which means that it cannot help improve the efficiency of the solar cell system. Thus, we do not need to increase the pulse number further when the hole appears. The pulse number corresponding to the formation of holes is set as the threshold for a fixed laser power.

Overall, for the microstructure formation as the pulse number increases while the laser power is fixed, the average height and interval distance of spikes increase near-linearly and a hole can be observed finally when the pulse number is large enough.

Furthermore, in order to show the detailed relation between the irradiated pulse number and average height of formed spikes, we measured the average height of the spikes fabricated under two gas pressures (66 and 80 kPa), in which the pulse number ranges from 300 to 2400 with the interval of 300. The corresponding results are shown in Fig. 4. It can be observed that for both pressures, the average height of the spikes increases approximately linearly as the pulse number increases. Differently, the average height and growth rate of the formed spikes under the pressure of 80 kPa are lower than under 66 kPa. This phenomenon can be explained by the detailed reaction process between SF_6 and silicon: under the irradiation of high-intensity femtosecond laser pulses, the gas medium SF_6 absorbs the energy of laser pulses and then can be dissociated to produce F atoms. The F atoms diffuse through the gas phase and react with silicon, forming volatile SiF_4,[21] and then a sharp morphology can be formed on the sample surface. For a given gas pressure, the produced F atoms is determined by irradiated laser fluence— each laser pulse corresponding to a fixed production ratio of F atoms, therefore the number of the F atoms is proportionally to the number of laser pulses. The F atoms react with silicon material, as a result, the average height of spikes increases approximately linearly as the increase of pulse number. However, for the dissociation of SF_6 under different gas pressures, there exist two contradictory factors: the higher the gas pressure, the higher the density of reactants, which is beneficial for the generation of F atoms. In contrast, the collisional deactivation can limit the dissociation of SF_6, which decreases exponentially with increasing pressure and then the decrease of the number of F atoms also occurs.[22] Therefore, there exists an optimal pressure for the silicon-gas reaction, in which the pressure of 70 kPa has been proved in the experiments.[23] Compared with 80 kPa, 66 kPa is closer to this optimal pressure of 70 kPa; then, the reaction between gas and silicon should be more vigorous. Thus, the corresponding average height and growth rate of spikes are all higher under 66 kPa.

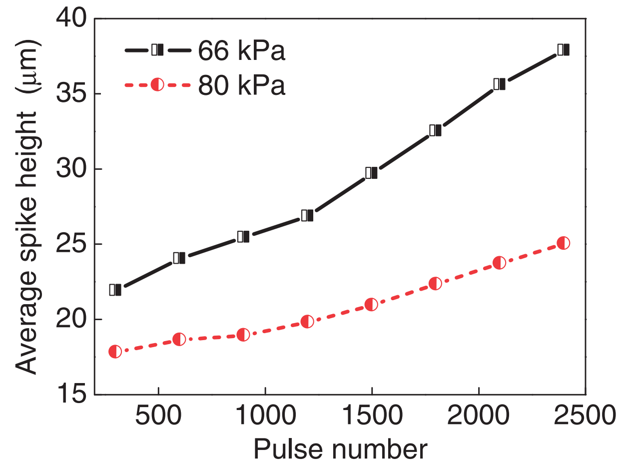

Fig. 4. Average height change of spikes as a function of pulse number under gas pressures of 66 kPa (black solid line) and 80 kPa (red dotted line).

We experimentally demonstrated that for the formation of microstructures as the pulse number increases while the laser power is fixed, both the average height and distance of spikes increase near-linearly. While when the pulse number exceeds a threshold for a fixed laser power, a hole can be observed and its depth continuously increases with the increase of pulse number. Furthermore, by comparing the average height of spikes formed under two different gas

 © 2013 The Japan Society of Applied Physics

Person-to-person distribution (up to 10 persons) by the author only. Not permitted for publication for institutional repositories or on personal Web sites.

pressures, we prove that the growth rate of the spike height is also dependent on the pressure of the filled gas. These results are important for promoting the development of the material fabrication for solar cells, sensors, optoelectronic detectors, and interrelated interdisciplinary subjects.

Acknowledgment This work was partly supported by the Leading Academic Discipline Project of Shanghai Municipal Government (S30502), "Chen Guang" Project of Shanghai Municipal Education Commission and Educational Development Foundation (12CG54), National Program on Key Basic Research Project of China (973 Program, 2012CB934203), National Natural Science Foundation of China (61007059, 11104186, 61138001, 11174207), the Major National Development Project of Scientific Instrument and Equipment (2011YQ150021, 2012YQ150092, 2012YQ140005), and the Shanghai Basic Research Key Project (12510502300).

1) M. Stubenrauch, M. Fischer, C. Kremin, S. Stoebenau, A. Albrecht, and O. Nagel: J. Micromech. Microeng. **16** (2006) S82.
2) T. Her, R. J. Finlay, C. Wu, S. Deliwala, and E. Mazur: Appl. Phys. Lett. **73** (1998) 1673.
3) A. Serpengüzel, A. Kurt, I. Inanç, J. Cary, and E. Mazur: J. Nanophotonics **2** (2008) 021770.
4) R. Younkin, J. E. Carey, E. Mazur, J. A. Levinson, and C. M. Friend: J. Appl. Phys. **93** (2003) 2626.
5) S. Moribe, A. Takeichi, J. Seki, N. Kato, K. Higuchi, K. Ueyama, K. Mizumoto, and T. Toyoda: Appl. Phys. Express **5** (2012) 112302.
6) H. Nakanishi, S. Fujiwara, K. Takayama, I. Kawayama, H. Murakami, and M. Tonouchi: Appl. Phys. Express **5** (2012) 112301.
7) W. Park: Laser Phys. Lett. **7** (2010) 93.
8) Z. Huang, J. E. Carey, M. Liu, E. Mazur, and J. C. Campbell: Appl. Phys. Lett. **89** (2006) 033506.
9) H. M. Branz, V. E. Yost, S. Ward, K. M. Jones, B. To, and P. Stradins: Appl. Phys. Lett. **94** (2009) 231121.
10) P. G. Maloney, P. Smith, V. King, C. Billman, M. Winkler, and E. Mazur: Appl. Opt. **49** (2010) 1065.
11) R. A. Myers, R. Farrell, A. M. Karger, J. E. Carey, and E. Mazur: Appl. Opt. **45** (2006) 8825.
12) Y. Peng, Y. Wen, D. S. Zhang, S. D. Luo, L. Chen, and Y. M. Zhu: Appl. Opt. **50** (2011) 4765.
13) C. H. Crouch, J. E. Carey, J. M. Warrender, M. J. Aziz, E. Mazur, and F. Y. Genin: Appl. Phys. Lett. **84** (2004) 1850.
14) V. Zorba, N. Boukos, I. Zergioti, and C. Fotakis: Appl. Opt. **47** (2008) 1846.
15) J. Zhu, Y. Shen, W. Li, X. Chen, G. Yin, D. Chen, and L. Zhao: Appl. Surf. Sci. **252** (2006) 2752.
16) J. D. Fowlkes, A. J. Pedraza, and D. H. Lowndes: Appl. Phys. Lett. **77** (2000) 1629.
17) Y. Peng, D. S. Zhang, H. Y. Chen, Y. Wen, S. D. Luo, L. Chen, K. J. Chen, and Y. M. Zhu: Appl. Opt. **51** (2012) 635.
18) M. Y. Shen, C. H. Crouch, J. E. Carey, and E. Mazur: Appl. Phys. Lett. **85** (2004) 5694.
19) M. A. Sheehy, L. Winston, J. E. Carey, C. M. Friend, and E. Mazur: Chem. Mater. **17** (2005) 3582.
20) B. R. Tull, J. E. Carey, E. Mazur, J. P. Mcdonald, and S. M. Yalisove: MRS Bull. **31** [08] (2006) 626.
21) T. J. Chuang: J. Chem. Phys. **74** (1981) 1453.
22) R. V. Ambartsumyan, Y. A. Gorokhov, V. S. Letokhov, G. N. Makarov, and A. A. Puretskii: Sov. Phys. JETP **44** (1976) 231.
23) S. Y. Liu, J. T. Zhu, Y. Liu, and Z. Zhao: Mater. Lett. **62** (2008) 3881.

 © 2013 The Japan Society of Applied Physics